First posted online on 21 October 2019 as 10.1242/dmm.042234
Access the most recent version at http://dmm.biologists.org/lookup/doi/10.1242/dmm.042234

Cellular mechanisms underlying *Pax3*-related neural tube defects and their prevention by folic acid

Sonia Sudiwala[a], Alexandra Palmer[b], Valentina Massa[c], Alan J. Burns, Louisa P.E. Dunlevy, Sandra C.P. De Castro, Dawn Savery, Kit-Yi Leung, Andrew J. Copp, Nicholas D.E. Greene*

UCL Great Ormond Street Institute of Child Health, University College London, London, WC1N 1EH, UK

Current address: [a] University of California San Francisco, USA; [b]Blizard Institute, Barts and the London School of Medicine and Dentistry, Queen Mary University of London, UK; [c] Department of Health Sciences, University of Milan, Italy.

*Corresponding author: NDE Greene, UCL Great Ormond Street Institute of Child Health. n.greene@ucl.ac.uk Tel: +44 2079052217 orcid.org/0000-0002-4170-5248

Keywords: folic acid/neural tube defects/Pax3/cell cycle

Summary Statement

Neural tube defects in a folic acid-responsive, folate-sensitive mouse model are associated with a localized proliferation defect in the neuroepithelium. Supplemental folic acid stimulates progression through S-phase of the cell cycle and corrects this abnormality.

Abstract

Neural tube defects (NTDs), including spina bifida and anencephaly, are among the most common birth defects worldwide but the underlying genetic and cellular causes are not well understood. Some NTDs are preventable by supplemental folic acid. However, the protective mechanism is unclear despite widespread use of folic acid supplements and implementation of food fortification in many countries. *Pax3* mutant (*splotch*; Sp^{2H}) mice provide a model in which NTDs are preventable by folic acid and exacerbated by maternal folate deficiency. Here, we found that cell proliferation was diminished in the dorsal neuroepithelium of mutant embryos, corresponding to the region of abolished Pax3 function. This was accompanied by premature neuronal differentiation in the prospective midbrain. Contrary to previous reports, we did not find evidence that increased apoptosis could underlie failed neural tube closure in *Pax3* mutant embryos, nor did inhibition of apoptosis prevent NTDs. These findings suggest that Pax3 functions to maintain the neuroepithelium in a proliferative, undifferentiated state allowing neurulation to proceed. NTDs in *Pax3* mutants were not associated with abnormal abundance of specific folates, nor prevented by formate, a one-carbon donor to folate metabolism. Supplemental folic acid restored proliferation in the cranial neuroepithelium. This effect was mediated by enhanced progression of the cell cycle from S- to G2-phase, specifically in the *Pax3*-mutant dorsal neuroepithelium. We propose that the cell cycle-promoting effect of folic acid compensates for loss of Pax3 and thereby prevents cranial NTDs.

Introduction

Neural tube defects (NTDs) such as anencephaly and spina bifida are among the most common birth defects worldwide, affecting more than 250,000 pregnancies every year (Copp et al., 2013; Zaganjor et al., 2016). Maternal use of supplemental folic acid (FA) prevents a proportion of NTDs (Berry et al., 1999; Czeizel and Dudás, 1992; MRC Vitamin Study Research Group, 1991) and FA food fortification programmes, which now exist in many countries, have generally been associated with a reduction in NTD prevalence, compared with historical pre-fortification frequencies (Berry et al., 2010; Castillo-Lancellotti et al., 2013). A key aim for public health efforts is now to ensure that women who may become pregnant achieve recommended daily intakes of FA, in order to lower NTD rates (Martinez et al., 2018). However, there is still a gap in our knowledge concerning the mechanism by which FA prevents NTDs in the developing embryo. FA is the synthetic form of folate, a term which refers to a group of molecules, based on a tetrahydrofolate (THF) backbone, that carry one-carbon units in folate one-carbon metabolism. FA is converted via dihydrofolate to THF, with subsequent addition of one-carbon groups derived principally from serine, glycine and formate (Tibbetts and Appling, 2010; Leung et al., 2017).

NTDs result from incomplete closure of the neural tube during embryonic development (Greene and Copp, 2014; Nikolopoulou et al., 2017). Among mouse genetic models, exencephaly and/or spina bifida arise in *splotch* mice, carrying mutations of the paired-box-domain-containing transcription factor Pax3 (Epstein et al., 1991; Greene et al., 2009). Notably, *Pax3* mutants (*Pax3*^{Sp2H}, *Pax3*^{Sp}) are among the very few models in which NTDs have been found to be both preventable by supplemental folic acid and exacerbated by maternal folate deficiency, imposed by diet and administration of antibiotic to remove folate-synthesizing gut bacteria (Burren et al., 2008; Fleming and Copp, 1998; Wlodarczyk et al., 2006). Hence, NTDs in this model are both folic acid-responsive and folate-sensitive. In addition to mutation of the *Pax3* gene itself, suppression of *Pax3* expression in mouse embryos is also proposed to contribute to NTDs induced by environmental factors, such as maternal diabetes (Fine et al., 1999; Machado et al., 2001) and polycyclic aromatic hydrocarbons (Lin et al., 2019).

Mutations of the human *PAX3* coding sequence have been identified in some individuals with NTDs (Hart and Miriyala, 2017) and may contribute to a minority of NTDs. Altered methylation of *PAX3* has also been identified in NTD cases, suggesting that altered expression could potentially play a contributory role (Lin et al., 2019).

Understanding the mechanisms by which *Pax3* loss of function prevents neural tube closure will not only give insight into possible causes of NTDs but may also provide an opportunity to better understand the means by which FA prevents NTDs. It has been proposed that Pax3-related NTDs (specifically the $Pax3^{Sp}$ allele) result from excess apoptosis: NTDs were prevented by genetic or pharmacological suppression of p53 function (Pani et al., 2002), leading to the hypothesis that Pax3 functions to suppress p53-dependent apoptosis in the neuroepithelium. A p53-dependent excess of apoptosis has also recently been proposed to underlie NTDs associated with zinc deficiency (Li et al., 2018). Both excess and insufficient apoptosis have been associated with exencephaly in other mouse mutants, although in most cases a causal relationship has not been definitively proven (Greene and Copp, 2014; Nikolopoulou et al., 2017).

Other studies of apoptosis in *splotch* ($Pax3^{Sp}$) embryos have produced differing findings. For example, increased TUNEL staining was reported in the neural tube at E10.5 (Pani et al., 2002), whereas no change in the number of pyknotic nuclei in the spinal neuroepithelium was detected at E9.5 (Kapron-Bras and Trasler, 1988). Moreover, whilst aberrant levels of apoptosis have been demonstrated in $Pax3^{Sp/Sp}$ and $Pax3^{Sp2H/Sp2H}$ mutants in the dermomyotome of the developing somites, increased apoptosis was not observed in the neural tube at E9.5 or later stages (Borycki et al., 1999; Mansouri et al., 2001). In the current study we sought to address the question of the possible contributory role of apoptosis to NTDs in the $Pax3^{Sp2H/Sp2H}$ model and to investigate other potential causative cellular abnormalities. Having identified a tissue-specific defect in cellular proliferation, we went on to ask whether this abnormality was corrected by folic acid supplementation in association with prevention of NTDs.

Results

NTDs in *Pax3* (*Sp^{2H}*) mutant embryos do not result from excess apoptosis

NTDs in *splotch* embryos result from a cell autonomous defect in the neuroepithelium (Goulding et al., 1991; Li et al., 1999). Therefore, if excess apoptosis is the cause of cranial NTDs in *Pax3* mutants, this should be detectable prior to and/or during closure of the cranial neuroepithelium which has not previously been examined.

The initiation of neural tube closure, at the hindbrain-cervical boundary (Closure 1; 5-6 somites; E8.5) and in the posterior forebrain (Closure 2; 9-10 somites; E9.0) occur similarly in *$Pax3^{Sp2H/Sp2H}$* embryos as in wild-type littermates. However, progression of 'zippering' forwards from Closure 1 and backwards from Closure 2 fails in those mutants that develop midbrain/hindbrain exencephaly (Fleming and Copp, 2000). In the current study, exencephaly, characterized by persistently open cranial neural folds, arose in 65% of *$Pax3^{Sp2H/Sp2H}$* mutants (n = 46), whereas all *$Pax3^{+/+}$* embryos (n = 54) completed closure by the 16 somite stage at E9.5 ($p<0.001$; Chi-square).

In *$Pax3^{+/+}$* and *$Pax3^{Sp2H/Sp2H}$* embryos, TUNEL-positive cells were detected in the rostral forebrain, the midline of the closed forebrain neural tube and in the hindbrain neural folds (Fig. 1A-F), corresponding to known sites of apoptosis in wild-type embryos (Massa et al., 2009; Mirkes et al., 2001). However, we did not observe an increase in the number or location of TUNEL-positive cells in the neural folds of *$Pax3^{Sp2H/Sp2H}$* embryos at any stage of closure in either the cranial or spinal region (Fig. 1; Fig. S1). Consistent with the results of TUNEL staining, the number of cleaved caspase-3 positive, apoptotic cells in the cranial neural folds did not differ between genotypes (Fig. 1G).

Although not supported by our TUNEL and cleaved caspase-3 analysis, we reasoned that if apoptosis is indeed causally related to *splotch* NTDs then direct inhibition of apoptosis would potentially rescue these defects. Therefore, as a complementary approach, embryos were cultured through the period encompassing cranial neurulation (40 hours from E8.5) in the presence of the pan-caspase inhibitor Z-VAD-FMK, which we previously showed to effectively suppress apoptosis in neurulation-stage embryos (Massa et al., 2009)(Fig. 2). Contrary to predictions, inhibiting apoptosis caused a dose-dependent increase in exencephaly incidence among *Pax3*$^{Sp2H/Sp2H}$ embryos. These defects were also observed among some heterozygotes, which are unaffected in the absence of Z-VAD-FMK (Fig. 2E). In addition, the posterior neuropore (PNP) length of *Sp*$^{2H/+}$ embryos treated with 200 µM Z-VAD-FMK was greater than among vehicle-treated controls, suggesting suppression of spinal neural tube closure (Table S1). Wild-type embryos were unaffected by the inhibitor. Moreover, there was no apparent effect of Z-VAD-FMK on viability, growth or developmental progression compared to vehicle-treated controls, showing that increased exencephaly frequency does not result from generalised non-specific teratogenicity (Table S1). Hence, inhibition of apoptosis does not prevent NTDs and may even interact with genetic mutation of *Pax3* to increase the susceptibility to NTDs in embryos carrying the *Sp*^{2H} allele. Overall, our data do not support the hypothesis that NTDs result from increased apoptosis in *Pax3* mutant embryos.

Pax3 mutation results in premature neuronal differentiation in the cranial neuroepithelium prior to failure of closure

We next asked whether the frequency of cranial NTDs in *Pax3*$^{Sp2H/Sp2H}$ embryos can be lowered by maternal treatment with pifithrin-α, as described for embryos homozygous for the *Sp* allele of *Pax3* (Pani et al., 2002). We found a lower frequency of cranial NTDs (Fig. 3A-B) among *Pax3*$^{Sp2H/Sp2H}$ offspring of pifithrin-α treated mice compared with untreated control litters (Fig. 3A; Table S2).

Pifithrin-α was originally identified in a screen for inhibitors of p53 (Murphy et al., 2004), suggesting this as a mode of action in *Pax3* mutants. Surprisingly however, among litters generated by intercross of *Pax3*$^{Sp2H/+}$; *Trp53*$^{+/-}$ mice we found no effect of p53 genotype on the susceptibility to NTDs in *Pax3*$^{Sp2H/Sp2H}$ embryos (Table 1). Cranial NTDs occurred among some *Trp53*$^{-/-}$ embryos that were wild-type, as predicted from previous reports (Sah et al., 1995), demonstrating effectiveness of the *Trp53* mutant allele. Moreover, *Trp53* mutation caused an increased rate of cranial NTDs in *Pax3*$^{Sp2H/+}$ heterozygotes (Table 1). Lack of replication of the reported NTD prevention in *Pax3*$^{Sp/Sp}$; *Trp53*$^{-/-}$ embryos (Pani et al., 2002) could potentially reflect an allele-specific difference between *Sp*, which primarily causes spinal NTDs, and *Sp*^{2H} which causes both cranial NTDs (approximately 60% of homozygotes) and almost fully penetrant spina bifida (Burren et al., 2008; Greene et al., 2009).

Possible cellular responses to p53 activity include not only apoptosis but also cell cycle arrest, senescence and differentiation (Vousden and Lane, 2007). Therefore, in view of the inconsistent findings with apoptosis inhibition, pifithrin-α usage and genetic knockout of p53, we asked whether cellular differentiation and/or cell cycle progression may be dysregulated in the neuroepithelium of *Pax3* mutant embryos.

In wild-type embryos, the onset of neuronal differentiation correlated closely with the timing of cranial neural tube closure at E9.5 (Fig. 3). Few cells were positive for the early neuronal marker, β-tubulin type III (TuJ1), in the midbrain neuroepithelium at the 13-15 somite stages, prior to closure (Fig. 3G, K). Neuronal differentiation then increased, concomitantly with completion of cranial neural tube closure, which is achieved in wild-type embryos by the 16 somite stage (Fig. 3K). In contrast, *Pax3*$^{Sp2H/Sp2H}$ embryos showed a pronounced shift in the timing of neuronal differentiation in the midbrain, compared with wild-type embryos, with 83% and 210% increases in the number of Tuj1 positive cells at the 14 and 15 somite stages, respectively (Fig. 3H, I, K). These supernumerary neuronal cells arose in the dorsal region of neuroepithelium corresponding to the Pax3 expression domain (Fig. 3C-D; Fig. S2), suggesting that differentiation occurred as a result of loss of Pax3 function. Hence, excess neuronal cells

were present in the midbrain neuroepithelium prior to failure of closure and at a stage when they are scarce in wild-type controls. Forebrain closure occurs successfully in *Pax3* mutant embryos, a region in which *Pax3* expression is weaker than at other axial levels of the neural tube (Fig. 3B-C). This region exhibited low numbers of Tuj1-positive cells at E9.5 with no difference between genotypes (Fig. 3E, F, L).

Among pifithrin-α treated embryos, concomitant with prevention of exencephaly in *Pax3*$^{Sp2H/Sp2H}$ embryos, there was a significant reduction in the number of TuJ1-positive cells in the midbrain neuroepithelium (Fig. 3J-K). Thus, our findings suggest that normalization of neural tube closure in *Pax3* mutant embryos following pifithrin-α treatment, may be mediated, not via prevention of p53-dependent apoptosis, but through suppression of premature neuronal differentiation.

Impaired cell cycle progression in *Pax3*-deficient neuroepithelium

We investigated the possibility that premature neuronal differentiation could be associated with altered proliferation in the neuroepithelium of *Pax3*$^{Sp2H/Sp2H}$ embryos. At neurulation stages, *Pax3*$^{Sp2H/Sp2H}$ embryos had comparable number of somites and crown-rump length to wild-type littermates, showing that there is no overall growth or developmental retardation (Table S3). However, we observed a significant deficit in the proportion of phospho-histone H3 (PHH3) labelled cells at late G2/M phase in the dorsal neural plate of *Pax3*$^{Sp2H/Sp2H}$ embryos (Fig. 3M). Hence, a dorsal-high, ventral-low proliferation differential was observed in the midbrain neuroepithelium of wild-type embryos at E9.5, consistent with findings in the spinal neural tube (Kim et al., 2007; McShane et al., 2015; Megason and McMahon, 2002), whereas this proliferation differential was absent in *Pax3*$^{Sp2H/Sp2H}$ mutants (Fig. 3M).

Failure of spinal neurulation is associated with diminished proliferation but not premature neuronal differentiation

The observation of premature neuronal differentiation and diminished proliferation in the dorsal cranial neuroepithelium at the stage of closure suggest potential causative mechanisms for cranial NTDs. We therefore asked whether comparable phenotypes were present in the spinal neural folds. Spina bifida occurs in almost all *Pax3*$^{Sp2H/Sp2H}$ embryos, and results from failure of PNP closure at E10.5. Measurements of PNP length showed that spinal neural tube closure was delayed from soon after initiation of closure with an enlarged PNP evident at E9.0 (12-13 somite stage) and becoming particularly prominent from E9.5 (14-16 somite stage) onwards (Fig. 4A; Fig. S2E). The PNP did not dramatically increase in size as development progresses, unlike in mutants such as *Grhl3*$^{-/-}$ (De Castro et al., 2018), indicating that closure progresses in *Pax3* mutants. However, this is at a diminished speed such that closure ultimately fails to be completed in the low spine.

Arguing against a primary effect in which the presence of neuronal cells causes spina bifida, abnormal neuronal differentiation was not apparent in the spinal neuroepithelium of *Pax3* mutants at E9.5. Neuronal differentiation proceeds in a rostro-caudal temporal wave and, in embryos of all genotypes, Tuj1 staining (whole mount and on sections) was apparent only in the closed neural tube rostral to the site of PNP zippering. Neurons were never observed in the open PNP region of *Pax3*$^{+/+}$ (n = 6), *Pax3*$^{Sp2H/Sp2H}$ (n = 7) or *Pax3*$^{Sp2H/+}$ (n = 7) embryos (Fig. 4B, C; Fig. S3). Moreover, the caudal axial level at which Tuj1-positive cells was detected in the closed neural tube did not differ between genotypes (Fig. S3).

As observed in the cranial region (Fig. 3M), the dorsal neuroepithelium of *Pax3*$^{Sp2H/Sp2H}$ embryos exhibited an apparent proliferation defect. Hence, at the 14-15 somite stage (E9.5), soon after delay of PNP closure become apparent, immunostaining for PHH3 at the rostral level of the PNP revealed a significant decrease in the proportion of cells at late G2/M-phase in the dorsal neural plate (Fig. 4D-E), corresponding to the region of *Pax3* loss of function (Fig. S2B). This proliferation deficit abolishes the dorsal-ventral proliferation difference that is present in wild-

type embryos at this stage (Fig. 4E; Fig. S4A-B) and led to a significant reduction in the number of cells in the neuroepithelium (Fig. 4F), including in both dorsal and ventral sub-regions (Fig. S4C-E). In parallel with this finding, the cross-sectional area of the neuroepithelium was diminished in *Pax3* mutants compared with wild-type embryos (Fig. 4G), as were the dorso-ventral height and medio-lateral width of the neural tube, but not their relative ratio (Fig. S4G-J). The significant deficit of cells and size of the *Pax3*-mutant neural plate, detected in 14-15 somite stage embryos, was still evident at the 19-20 somite stage (Fig. 4F-G, Fig. S4). These findings show that suppression of PNP closure is associated with a proliferation defect in the dorsal neuroepithelium.

Overall, *Pax3* loss of function in the spinal region causes diminished proliferation without induction of neuronal differentiation. It seems likely that Pax3 has comparable functions at cranial and spinal levels. Hence, the effect of Pax3 on the balance between proliferation and differentiation in the cranial region, where the neuroepithelium is primed to differentiate, may be principally mediated through regulation of cell cycle progression rather than direct inhibition of differentiation.

In *Pax3* mutants, folic acid acts to increase cell proliferation by promoting S-phase to G2 progression

Splotch (*Pax3*^{Sp2H}) was the first mouse model in which NTDs were found to be preventable by supplemental folic acid (FA) (Fleming and Copp, 1998), but as in human NTDs the protective mechanism has not been defined. FA is reduced via dihydrofolate to tetrahydrofolate (THF), which acts to carry one-carbon groups in folate one-carbon metabolism (FOCM), a key function of which is to provide one-carbon units for nucleotide biosynthesis. Our previous analysis showed no effect of *Pax3*^{Sp2H} genotype on embryonic folate content at neurulation stages (Burren et al., 2008). Here, mass spectrometry-based analysis of the individual folate species which comprise FOCM did not reveal significant perturbation in their relative abundance in *Pax3*$^{Sp2H/Sp2H}$ embryos compared with wild-type (Fig. 5A). This is consistent with our finding that the relative abundance of s-adenosylhomocysteine and s-adenosylmethionine did not differ

with *Pax3*^{Sp2H} genotype (Burren et al., 2008). Moreover, unlike loss of function mutants of the mitochondrial FOCM components: Mthfd1L and Gldc or the mitochondrial folate transporter SLC25A32 (Momb et al., 2013; Pai et al., 2015; Leung et al., 2017; Kim et al., 2018), NTDs were not prevented by maternal supplementation with formate, a one–carbon donor, in *Pax3* mutants (Table S4).

Cranial neurulation appears highly sensitive to disturbance of cellular proliferation, with exencephaly often being induced by teratogens that cause generalised retardation of embryonic growth or developmental progression (Copp, 2005). Together with our finding of a proliferation defect in the Pax3-deficient cranial and spinal neuroepithelium, this prompted the question of whether FA status impacts cell proliferation in developing *Pax3*$^{Sp2H/Sp2H}$ embryos. Indeed, FA is required for proliferation of cultured neural progenitor cells (Ichi et al., 2010; Ichi et al., 2011). We therefore carried out further analysis of cell cycle progression in the *Pax3* mutant neural plate in order to determine whether maternal FA treatment could influence cell cycle progression. Dams were treated with FA using the protocol that we found to reduce the frequency of cranial NTDs among *Pax3*$^{Sp2H/Sp2H}$ offspring (Burren et al., 2008; Fleming and Copp, 1998). Embryos were analysed during the period of cranial neurulation at E9.5 (14-15 somite stage), with a pulse of BrdU preceding embryo collection to allow analysis of cell cycle progression in the midbrain neuroepithelium (Fig. 5B).

The proportion of cells in G2 and M-phase of the cell cycle were analysed on the basis of the characteristic appearance of PHH3 imunostaining (de Castro et al., 2012). A lower proportion of non-mitotic PHH3-positive (early G2-late G2) cells were present in the dorsal neuroepithelium of *Pax3*$^{Sp2H/Sp2H}$ embryos compared with +/+ littermates (Fig. 5C), corresponding with the observed deficit of cells at late G2/M phase (Fig. 3M). In contrast, the mitotic (M-phase) population did not differ between genotypes (Fig. 5D). Interestingly, there was a small but significantly higher proportion of G2 phase cells in the ventral neuroepithelium of *Pax3* mutant compared with +/+ embryos, which suggests a possible non-cell autonomous effect of Pax3 loss of function.

The BrdU labelling index (reporting cells in S-phase) was also significantly diminished in the dorsal neuroepithelium of *Pax3*$^{Sp2H/Sp2H}$ embryos (Fig. 5E), whereas the ventral region did not differ from wild-type (Fig. 5E). Hence, both BrdU labelling and PHH3 immunostaining showed the presence of a dorsal-high to ventral-low proliferation differential in wild-type embryos that is absent, or even reversed, in *Pax3* mutants (Fig. 5D-E).

FA treatment had a striking effect on cell cycle parameters, particularly in the dorsal midbrain neuroepithelium of *Pax3*$^{Sp2H/Sp2H}$ embryos where an FA-induced increase in the proportion of PHH3-positive, G2-phase cells was observed (Fig. 5C). Similarly, while FA did not significantly alter the proportion of S-phase, BrdU-labelled cells there was a trend towards increased labelling in all regions (Fig. 5E). Most notably, in FA-treated *Pax3*$^{Sp2H/Sp2H}$ embryos, we observed a significant increase in the proportion of double-positive BrdU/PHH3 cells; i.e. cells that were in S phase during the pulse of BrdU labelling and then progressed into G2 by the time of embryo collection (Fig. 5F). Hence, the rate of transition from S-phase to G2 was increased by supplemental FA.

In the dorsal and ventral neuroepithelium of *Pax3*$^{+/+}$ embryos, FA treatment led to non-significant trends towards increased labelling for both PHH3 (Fig. 5C) and BrdU (Fig. 5E). As a result, the dorsal-ventral proliferation differential was absent in FA-treated +/+ embryos. In contrast, the proportion of cells in M-phase did not differ with FA treatment in either *Pax3* genotype (Fig. 5D).

Discussion

The *Pax3* mutant (*Sp*^{2H}) mouse provides a model in which to investigate the cause of NTDs that are sensitive to folate deficiency and responsive to prevention by FA. Analysis of apoptosis markers, together with lack of NTD prevention by inhibition of apoptosis, are incompatible with the idea that increased cell death contributes to failure of neural tube closure. Instead, our findings suggest that Pax3 is required for cell cycle progression and suppression of neuronal differentiation in the dorsal neuroepithelium until completion of cranial neural tube closure.

The close correlation between onset of neuronal differentiation and completion of cranial neural tube closure that is observed in wild-type embryos is lost in *Pax3* mutants. Consistent with these observations, anti-sense down-regulation of *Pax3* in cultured neuronal ND7 cells resulted in morphological differentiation, without apparent cell death (Reeves et al., 1999). Similarly, during melanogenesis, Pax3 induces the melanocyte fate but acts to repress terminal differentiation until additional differentiation signals are present (Lang et al., 2005). Moreover, during myogenesis *Pax3* is required in muscle progenitors but must be down-regulated for myoblast differentiation (Goljanek-Whysall et al., 2011). Thus, in different cellular contexts, including the neuroepithelium, Pax3 may function to maintain committed progenitor cells in an undifferentiated, proliferative state until an appropriate developmental stage.

The relationship between *Pax3* mutation, cell cycle regulation and folate status is intriguing. Function of FOCM depends on adequate abundance of the tetrahydrofolate (THF) 'backbone' (from maternal diet and/or microbiota) and supply of one-carbon (1C) units. Supplemental FA can enhance supply of THF but does not carry a 1C unit. During neurulation the primary requirement for 1C units is met by catabolism of serine and glycine in mitochondrial FOCM (Leung et al., 2017; Tibbetts and Appling, 2010). This generates formate that is transferred to cytoplasmic FOCM in which the intermediates 5,10-methylene THF and 10-formyl THF act as the 1C donors in thymidylate and purine biosynthesis, respectively. Conditions of folate-deficiency further impose a requirement for serine-dependent generation of 5,10-methylene THF by the action of SHMT1 (Beaudin et al., 2011), acting in the cytoplasm and/or nucleus (Herbig et al., 2002; MacFarlane et al., 2011).

Pax3 genotype does not affect embryonic folate content at neurulation stages (Burren et al., 2008) or the relative proportion of different folate intermediates (the current study). This contrasts with mouse embryos carrying genetic defects in FOCM-associated enzymes such as *Mthfr* (Leung et al., 2017) and *Gldc* (Pai et al., 2015) or with methotrexate exposure (a FOCM inhibitor)(Leung et al., 2013a). Unlike in *Pax3* mutants, NTDs resulting from disruption of the 1C supply from mitochondrial FOCM (e.g. by mutation of Gldc or Amt) are neither FA-preventable

nor responsive to folate deficiency (Narisawa et al., 2012; Pai et al., 2015). Furthermore, while NTDs in *Gldc* and *Mthfd1L* null embryos are preventable by maternal supplementation with formate as a 1C donor (Leung et al., 2017; Momb et al., 2013; Pai et al., 2015), we found no apparent protective effect of this treatment in *Pax3* mutants. These findings highlight the potential for non-equivalent mechanisms underlying FA-mediated prevention of NTDs compared with prevention by 1C donors (e.g. formate) of NTDs resulting from disruption of FOCM.

Overall, it appears unlikely that NTDs in *Pax3* (*splotch*) embryos result from a deficit in folate uptake, 1C supply or interconversion of folate intermediates in FOCM. Significantly however, *Pax3* mutant embryos and embryonic fibroblasts preferentially use the nucleotide salvage pathway over *de novo* thymidylate biosynthesis, suggesting a possible impairment of FOCM that could underlie sensitivity to maternal folate status (Beaudin et al., 2011; Burren et al., 2008; Fleming and Copp, 1998). Moreover, the mutual NTD-exacerbating pairwise interactions of folate deficiency, *Shmt1* loss of function and *Pax3* mutation further implicate thymidylate synthase as an FA-sensitive process for neural tube closure (Beaudin et al., 2011; Burren et al., 2008; Martiniova et al., 2015). For example, folate deficiency or *Pax3* mutation can cause NTDs in *Shmt1* null embryos, which do not exhibit NTDs on a folate-replete diet (Beaudin et al., 2011). While the apparent deficit of *de novo* thymidylate synthesis in $Pax3^{Sp2H}$ mutants, under normal dietary conditions, is not due to a limiting pool of 5,10-methylene THF it may instead relate to post-transcriptional down-regulation of thymidylate synthase, as found in $Pax3^{Sp}$ mutant embryos (Beaudin et al., 2011). A lowering of THF availability in folate deficient conditions could then further suppress thymidylate synthesis and exacerbate NTDs. This would also be consistent with the increased frequency of *Pax3*-related NTDs caused by loss of function of Shmt1, whose translocation to the nucleus favours use of 5,10-methylene THF in thymidylate synthesis over reduction to 5-methyl THF for methylation of homocysteine (Herbig et al., 2002).

We previously found that maternal dietary folate deficiency limits embryonic growth and developmental progression of wild-type and *Pax3* mutant embryos without dissociating these parameters (Burren et al., 2008). Here, we find that supplemental FA stimulates cell cycle progression and that this effect is mediated via an increased rate of transition through S-phase and into G2-phase. An effect of FA in the DNA synthesis phase of the cell cycle correlates with a proposed mechanism of FA action in stimulating thymidylate biosynthesis.

Notably, the effect of FA in driving cell cycle progression was greatest in *Pax3* mutant regions, such that the overall effect was to normalize the dorsal-ventral proliferation gradient in $Pax3^{Sp2H/Sp2H}$ embryos. It appears that dorsal proliferation *per se*, as opposed to the dorsal-ventral gradient specifically, is associated with NTD prevention as FA-treated wild-type embryos no longer exhibit a proliferation gradient, but all complete closure. The particular requirement for cellular folate in the dorsal neuroepithelium is highlighted by the notable dorsal (overlapping the Pax3 expression domain) versus ventral enrichment of mRNA for the folate receptor, *Folr1*, (Saitsu et al., 2003), whose knockout also causes NTDs (Piedrahita et al., 1999). Overall, we hypothesise that supplemental FA contributes to neural tube closure by promoting S-phase cell cycle progression, particularly in the neuroepithelial component of the dorsal neural folds.

Materials and Methods

Mice and collection of embryos

Pax^{Sp2H} (*Sp*^{2H}; *splotch*) mice were maintained as a closed, random-bred (heterozygous with wild-type) colony. The *Sp*^{2H} mutation is carried on a mixed background which includes CBA/Ca, 101 and C3H/He. Experimental litters were generated by intercross of heterozygous mice. Embryos were genotyped by PCR of genomic DNA (Conway et al., 1997). To generate mice lacking p53, $Trp53^{flox/+}$ (Jonkers et al., 2001) were used to generate $Trp53^{+/-}$ heterozygotes for intercross to $Pax3^{Sp2H}$. The $Pax3^{cre}$ allele was used as a null allele in crosses with the p53 null allele (Engleka et al., 2005).

Pifithrin-α (Calbiochem) treatment at a dose of 2.2 mg/kg was achieved by intra-peritoneal injection with 0.22 mg/ml solution (diluted with PBS from a 5 mg/ml stock in sterile DMSO), at E8.5 and 9.5 (Pani et al., 2002). Folic acid (20 mg/kg) was administered by intra-peritoneal injection of dams at E7.5, 8.5 and 9.5, using a dose that we have found to lower frequency of NTDs (Burren et al., 2008; Fleming and Copp, 1998). Embryos were collected 3 hours after the final injection. Formate treatment was by addition of sodium formate (30 mg/ml) in the drinking water of the dam from E0.5 until collection of litters (Pai et al., 2015). Litters were dissected from the uterus in Dulbecco's Modified Eagle's Medium (DMEM) containing 10% fetal calf serum. Embryos were rinsed in phosphate buffered saline (PBS) and fixed in 4% paraformaldehyde. Embryos were dehydrated in a methanol series and stored at -20°C prior to *in situ* hybridisation or TUNEL analysis.

For immunohistochemistry, BrdU (Invitrogen) was administered by maternal intraperitoneal injection at 50 mg/kg from a stock solution of 10 mg/ml. Litters were collected after 15 minutes, embryos explanted in ice-cold DMEM, immediately fixed in 4% paraformaldehyde, dehydrated through an ethanol series and processed for wax embedding.

Whole embryo culture

Embryos were explanted at E8.5 leaving the yolk sac and ectoplacental cone intact and cultured for 40 hours in rat serum at 38°C (Dunlevy et al., 2006; Pryor et al., 2012). Stock solutions of 50 and 100 mM Z-VAD-FMK (Sigma-Aldrich) in dimethylsulfoxide (DMSO) were added to cultures as 0.2% (v/v) additions. An equivalent volume of vehicle was added to control cultures, and embryos were randomly allocated to treatment groups.

TUNEL labeling

TdT-mediated dUTP-biotin nick end labelling (TUNEL) of whole embryos (Dunlevy et al., 2006) was performed on a minimum of 8 embryos of each genotype at E8.5, E9.0, E9.5 and E10.5.

Whole mount in situ hybridisation (WMISH)

Whole mount *in situ* hybridisation (De Castro et al., 2018) was performed using sense and anti-sense digoxygenin-labelled riboprobes for *Pax3* (Conway et al., 1997), generated using a digoxygenin RNA labelling kit (Roche) and purified on Chroma spin columns (Clontech).

Immunohistochemistry

Immunostaining using antibodies for PHH3 (06-570 Merck Millipore) and activated caspase-3 (Cell Signalling Technology) was performed on paraffin-embedded coronal (cranial) or transverse (spinal) sections. Numbers of positive cells were counted in defined areas, blind to genotype (Dunlevy et al., 2006). The number of positive cells per section was normalised to the area of neuroepithelium (cells/1000 μm^2) or the total number of neuroepithelial cells on the section as detected by DAPI staining (% labelling).

Double staining for PHH3 and BrdU was performed following deparaffinising of slides by HistoClear. Sections were rehydrated through an ethanol series and antigen retrieval was performed in 0.01 M citric acid (pH 6.0). After washing in phosphate buffered saline (PBS), 0.1% Triton-X100, slides were blocked in 5% sheep serum, 0.15% glycine, 2% BSA, followed by addition of anti-PHH3 (1:300). Secondary antibody was Alexa Fluor 568 (A11077, Life Technologies), diluted 1:500 in blocking solution. Nuclear stain was 4',6-diamidino-2-phenylindole (DAPI), diluted in PBS (1: 10,000). After post-fixation in 4% PFA, slides were incubated in 1 M HCl, followed by 2 M HCl, to expose the BrdU antigen, and neutralised by washing in 0.1 M sodium borate (pH 8.5). Slides were blocked in 10% sheep serum and incubated with anti-BrdU (347583, BD Bioscience; 1:100). After incubation with secondary antibody (Alexa Fluor 488; A11070, Life Technologies; 1:500), slides were mounted (12.5% Mowiol 4-88 (Sigma-Aldrich), 0.2 M Tris base, 0.2 M Tris-HCl, 30% glycerol, pH 6.8). Images were acquired on an inverted LSM710 confocal microscope (Zeiss).

For TuJ1 (β-tubulin type III) staining, 15 µm coronal cryosections were prepared (Burns and Douarin, 1998). Sections were blocked (PBS, 10% heat-inactivated sheep serum, 0.1% Triton-X-100) and treated with primary antibodies against TuJ1 (1:1000 in blocking solution, BAbCO) or Pax3 (1:50, ATCC), followed by secondary antibody (goat anti-mouse Alexa-488, 1: 500, Southern Biotech). Sections were mounted in Vectashield with DAPI (Vector Laboratories). The number of TuJ1-positive cells in 3 adjacent matched sections of forebrain and midbrain was counted for each embryo.

For whole mount immunostaining embryos were fixed in methanol/DMSO (4:1) and incubated in methanol/DMSO/30% hydrogen peroxide (4:1:1). Embryos were blocked in PBS containing 2% non-fat dried milk, 0.5% Triton X-100 and 10% sheep serum, and then incubated in the same solution with antibody to TuJ1 (1:1000) followed by secondary antibody (Alexa-488 donkey anti-mouse; 1:500, Invitrogen).

Analysis of folates by mass spectrometry

Analysis of multiple folates was performed by UPLC-MS/MS as described previously (Leung et al., 2017; Pai et al., 2015). Folates were measured by multiple reaction monitoring (MRM) with optimised cone voltage and collision energy for precursor and product ions as described (Cabreiro et al., 2013; Leung et al., 2013b) (Leung et al., 2013a).

Statistical analysis was performed using Sigmastat version 3.5 (Systat Software).

Competing interests: None

Funding

This study was supported by funding from the Medical Research Council (J003794 and K02274), Wellcome Trust (087525), Child Health Research Charitable Incorporated Organisation, Great Ormond Street Children's Charity and Newlife Foundation. Research was supported by the NIHR Great Ormond Street Hospital Biomedical Research Centre.

Author contributions: Study design, NDEG, AJC; Investigation, NDEG, SS, AP, VM, AJB, LPED, SDC, DS, KYL; Writing, NDEG, SS; Editing, NDEG, AJC.

References

Beaudin,A.E., Abarinov,E.V., Noden,D.M., Perry,C.A., Chu,S., Stabler,S.P., Allen,R.H., and Stover,P.J. (2011). Shmt1 and de novo thymidylate biosynthesis underlie folate-responsive neural tube defects in mice. *Am. J. Clin. Nutr.* **93,** 789-798.

Berry,R.J., Bailey,L., Mulinare,J., and Bower,C. (2010). Fortification of flour with folic acid. *Food Nutr. Bull.* **31,** S22-S35.

Berry,R.J., Li,Z., Erickson,J.D., Li,S., Moore,C.A., Wang,H., Mulinare,J., Zhao,P., Wong,L.Y.C., Gindler,J. et al. (1999). Prevention of neural-tube defects with folic acid in China. *N. Engl. J. Med.* **341,** 1485-1490.

Borycki,A.G., Li,J., Jin,F.Z., Emerson,C.P., Jr., and Epstein,J.A. (1999). Pax3 functions in cell survival and in *Pax7* regulation. *Development* **126,** 1665-1674.

Burns,A.J. and Douarin,N.M. (1998). The sacral neural crest contributes neurons and glia to the post-umbilical gut: spatiotemporal analysis of the development of the enteric nervous system. *Development* **125,** 4335-4347.

Burren,K.A., Savery,D., Massa,V., Kok,R.M., Scott,J.M., Blom,H.J., Copp,A.J., and Greene,N.D.E. (2008). Gene-environment interactions in the causation of neural tube defects: folate deficiency increases susceptibility conferred by loss of *Pax3* function. *Hum. Mol. Genet.* **17,** 3675-3685.

Cabreiro,F., Au,C., Leung,K.Y., Vergara-Irigaray,N., Cocheme,H.M., Noori,T., Weinkove,D., Schuster,E., Greene,N.D., and Gems,D. (2013). Metformin retards aging in C. elegans by altering microbial folate and methionine metabolism. *Cell* **153,** 228-239.

Castillo-Lancellotti,C., Tur,J.A., and Uauy,R. (2013). Impact of folic acid fortification of flour on neural tube defects: a systematic review. *Public Health Nutr.* **16,** 901-911.

Conway,S.J., Henderson,D.J., and Copp,A.J. (1997). *Pax3* is required for cardiac neural crest migration in the mouse: evidence from the *splotch* (Sp^{2H}) mutant. *Development* **124,** 505-514.

Copp,A.J. (2005). Neurulation in the cranial region - normal and abnormal. *J. Anat.* **207,** 623-635.

Copp,A.J., Stanier,P., and Greene,N.D. (2013). Neural tube defects: recent advances, unsolved questions, and controversies. *Lancet Neurol.* **12,** 799-810.

Czeizel,A.E. and Dudás,I. (1992). Prevention of the first occurrence of neural-tube defects by periconceptional vitamin supplementation. *N. Engl. J. Med.* **327,** 1832-1835.

de Castro,S.C., Malhas,A., Leung,K.Y., Gustavsson,P., Vaux,D.J., Copp,A.J., and Greene,N.D. (2012). Lamin b1 polymorphism influences morphology of the nuclear envelope, cell cycle progression, and risk of neural tube defects in mice. *PLoS Genet.* **8,** e1003059.

De Castro,S.C.P., Hirst,C.S., Savery,D., Rolo,A., Lickert,H., Andersen,B., Copp,A.J., and Greene,N.D.E. (2018). Neural tube closure depends on expression of Grainyhead-like 3 in multiple tissues. *Dev. Biol.* **435,** 130-137.

Dunlevy,L.P.E., Burren,K.A., Mills,K., Chitty,L.S., Copp,A.J., and Greene,N.D.E. (2006). Integrity of the methylation cycle is essential for mammalian neural tube closure. *Birth Defects Research (Part A)* **76,** 544-552.

Engleka,K.A., Gitler,A.D., Zhang,M.Z., Zhou,D.D., High,F.A., and Epstein,J.A. (2005). Insertion of Cre into the *Pax3* locus creates a new allele of *Splotch* and identifies unexpected *Pax3* derivatives. *Dev. Biol.* **280,** 396-406.

Epstein,D.J., Vekemans,M., and Gros,P. (1991). splotch (Sp^{2H}), a mutation affecting development of the mouse neural tube, shows a deletion within the paired homeodomain of Pax-3. *Cell* **67,** 767-774.

Fine,E.L., Horal,M., Chang,T.I., Fortin,G., and Loeken,M.R. (1999). Evidence that elevated glucose causes altered gene expression, apoptosis, and neural tube defects in a mouse model of diabetic pregnancy. *Diabetes* **48,** 2454-2462.

Fleming,A. and Copp,A.J. (1998). Embryonic folate metabolism and mouse neural tube defects. *Science* **280,** 2107-2109.

Fleming,A. and Copp,A.J. (2000). A genetic risk factor for mouse neural tube defects: defining the embryonic basis. *Hum. Mol. Genet.* **9,** 575-581.

Goljanek-Whysall,K., Sweetman,D., Abu-Elmagd,M., Chapnik,E., Dalmay,T., Hornstein,E., and Munsterberg,A. (2011). MicroRNA regulation of the paired-box transcription factor Pax3 confers robustness to developmental timing of myogenesis. *Proc. Natl. Acad. Sci. U. S. A* **108,** 11936-11941.

Goulding,M.D., Chalepakis,G., Deutsch,U., Erselius,J.R., and Gruss,P. (1991). Pax-3, a novel murine DNA binding protein expressed during early neurogenesis. *EMBO J.* **10,** 1135-1147.

Greene,N.D. and Copp,A.J. (2014). Neural tube defects. *Annu. Rev. Neurosci.* **37,** 221-242.

Greene,N.D., Massa,V., and Copp,A.J. (2009). Understanding the causes and prevention of neural tube defects: Insights from the splotch mouse model. *Birth Defects Res. A Clin Mol. Teratol.* **85,** 322-330.

Hart,J. and Miriyala,K. (2017). Neural tube defects in Waardenburg syndrome: A case report and review of the literature. *Am. J. Med. Genet. A* **173,** 2472-2477.

Herbig,K., Chiang,E.P., Lee,L.R., Hills,J., Shane,B., and Stover,P.J. (2002). Cytoplasmic serine hydroxymethyltransferase mediates competition between folate-dependent deoxyribonucleotide and S-adenosylmethionine biosyntheses. *J. Biol. Chem.* **277,** 38381-38389.

Ichi,S., Costa,F.F., Bischof,J.M., Nakazaki,H., Shen,Y.W., Boshnjaku,V., Sharma,S., Mania-Farnell,B., McLone,D.G., Tomita,T. et al. (2010). Folic acid remodels chromatin on Hes1 and Neurog2 promoters during caudal neural tube development. *J. Biol. Chem.* **285,** 36922-36932.

Ichi,S., Nakazaki,H., Boshnjaku,V., Singh,R.M., Mania-Farnell,B., Xi,G., McLone,D.G., Tomita,T., and Mayanil,C.S. (2012). Fetal Neural Tube Stem Cells from Pax3 Mutant Mice Proliferate, Differentiate, and Form Synaptic Connections When Stimulated with Folic Acid. *Stem Cells Dev.* **21,** 321-330.

Jonkers,J., Meuwissen,R., van der Gulden,H., Peterse,H., van,d., V, and Berns,A. (2001). Synergistic tumor suppressor activity of BRCA2 and p53 in a conditional mouse model for breast cancer. *Nat. Genet.* **29,** 418-425.

Kapron-Bras,C.M. and Trasler,D.G. (1988). Histological comparison of the effects of the splotch gene and retinoic acid on the closure of the mouse neural tube. *Teratology* **37,** 389-399.

Kim,J., Lei,Y., Guo,J., Kim,S.E., Wlodarczyk,B.J., Cabrera,R.M., Lin,Y.L., Nilsson,T.K., Zhang,T., Ren,A. et al. (2018). Formate rescues neural tube defects caused by mutations in Slc25a32. *Proc. Natl. Acad. Sci. U. S. A* **115,** 4690-4695.

Kim,T.H., Goodman,J., Anderson,K.V., and Niswander,L. (2007). Phactr4 regulates neural tube and optic fissure closure by controlling PP1-, Rb-, and E2F1-regulated cell-cycle progression. *Dev. Cell* **13,** 87-102.

Lang,D., Lu,M.M., Huang,L., Engleka,K.A., Zhang,M.Z., Chu,E.Y., Lipner,S., Skoultchi,A., Millar,S.E., and Epstein,J.A. (2005). Pax3 functions at a nodal point in melanocyte stem cell differentiation. *Nature* **433,** 884-887.

Leung,K.Y., De Castro,S.C., Cabreiro,F., Gustavsson,P., Copp,A.J., and Greene,N.D. (2013a). Folate metabolite profiling of different cell types and embryos suggests variation in folate one-carbon metabolism, including developmental changes in human embryonic brain. *Mol. Cell Biochem.* **378,** 229-236.

Leung,K.Y., de Castro,S.C., Cabreiro,F., Gustavsson,P., Copp,A.J., and Greene,N.D. (2013b). Folate metabolite profiling of different cell types and embryos suggests variation in folate one-carbon metabolism, including developmental changes in human embryonic brain. *Mol. Cell Biochem.* **378,** 229-236.

Leung,K.Y., Pai,Y.J., Chen,Q., Santos,C., Calvani,E., Sudiwala,S., Savery,D., Ralser,M., Gross,S.S., Copp,A.J. et al. (2017). Partitioning of One-Carbon Units in Folate and Methionine Metabolism Is Essential for Neural Tube Closure. *Cell Rep.* **21,** 1795-1808.

Li,H., Zhang,J., and Niswander,L. (2018). Zinc deficiency causes neural tube defects through attenuation of p53 ubiquitylation. *Development* **145**.

Li,J., Liu,K.C., Jin,F., Lu,M.M., and Epstein,J.A. (1999). Transgenic rescue of congenital heart disease and spina bifida in Splotch mice. *Development* **126,** 2495-2503.

Lin,S., Ren,A., Wang,L., Santos,C., Huang,Y., Jin,L., Li,Z., and Greene,N.D.E. (2019). Aberrant methylation of Pax3 gene and neural tube defects in association with exposure to polycyclic aromatic hydrocarbons. *Clin. Epigenetics.* **11,** 13.

MacFarlane,A.J., Anderson,D.D., Flodby,P., Perry,C.A., Allen,R.H., Stabler,S.P., and Stover,P.J. (2011). Nuclear localization of de novo thymidylate biosynthesis pathway is required to prevent uracil accumulation in DNA. *J. Biol. Chem.* **286,** 44015-44022.

Machado,A.F., Zimmerman,E.F., Hovland,D.N., Jr., Weiss,R., and Collins,M.D. (2001). Diabetic embryopathy in C57BL/6J mice - Altered fetal sex ratio and impact of the splotch allele. *Diabetes* **50,** 1193-1199.

Mansouri,A., Pla,P., Larue,L., and Gruss,P. (2001). *Pax3* acts cell autonomously in the neural tube and somites by controlling cell surface properties. *Development* **128,** 1995-2005.

Martinez,H., Weakland,A.P., Bailey,L.B., Botto,L.D., De-Regil,L.M., and Brown,K.H. (2018). Improving maternal folate status to prevent infant neural tube defects: working group conclusions and a framework for action. *Ann. N. Y. Acad. Sci.* **1414,** 5-19.

Martiniova,L., Field,M.S., Finkelstein,J.L., Perry,C.A., and Stover,P.J. (2015). Maternal dietary uridine causes, and deoxyuridine prevents, neural tube closure defects in a mouse model of folate-responsive neural tube defects. *Am. J. Clin. Nutr.* **101,** 860-869.

Massa,V., Savery,D., Ybot-Gonzalez,P., Ferraro,E., Rongvaux,A., Cecconi,F., Flavell,R.A., Greene,N.D.E., and Copp,A.J. (2009). Apoptosis is not required for mammalian neural tube closure. *Proc. Natl. Acad. Sci. U. S. A* **106,** 8233-8238.

McShane,S.G., Mole,M.A., Savery,D., Greene,N.D., Tam,P.P., and Copp,A.J. (2015). Cellular basis of neuroepithelial bending during mouse spinal neural tube closure. *Dev. Biol.* **404,** 113-124.

Megason,S.G. and McMahon,A.P. (2002). A mitogen gradient of dorsal midline Wnts organizes growth in the CNS. *Development* **129,** 2087-2098.

Mirkes,P.E., Little,S.A., and Umpierre,C.C. (2001). Co-localization of active caspase-3 and DNA fragmentation (TUNEL) in normal and hyperthermia-induced abnormal mouse development. *Teratology* **63,** 134-143.

Momb,J., Lewandowski,J.P., Bryant,J.D., Fitch,R., Surman,D.R., Vokes,S.A., and Appling,D.R. (2013). Deletion of Mthfd1l causes embryonic lethality and neural tube and craniofacial defects in mice. *Proc. Natl. Acad. Sci. U. S. A* **110,** 549-554.

MRC Vitamin Study Research Group (1991). Prevention of neural tube defects: Results of the Medical Research Council Vitamin Study. *Lancet* **338,** 131-137.

Murphy,P.J., Galigniana,M.D., Morishima,Y., Harrell,J.M., Kwok,R.P., Ljungman,M., and Pratt,W.B. (2004). Pifithrin-alpha inhibits p53 signaling after interaction of the tumor suppressor protein with hsp90 and its nuclear translocation. *J. Biol. Chem.* **279,** 30195-30201.

Narisawa,A., Komatsuzaki,S., Kikuchi,A., Niihori,T., Aoki,Y., Fujiwara,K., Tanemura,M., Hata,A., Suzuki,Y., Relton,C.L. et al. (2012). Mutations in genes encoding the glycine cleavage system predispose to neural tube defects in mice and humans. *Hum. Mol. Genet.* **21,** 1496-1503.

Nikolopoulou,E., Galea,G.L., Rolo,A., Greene,N.D., and Copp,A.J. (2017). Neural tube closure: cellular, molecular and biomechanical mechanisms. *Development* **144,** 552-566.

Pai,Y.J., Leung,K.Y., Savery,D., Hutchin,T., Prunty,H., Heales,S., Brosnan,M.E., Brosnan,J.T., Copp,A.J., and Greene,N.D. (2015). Glycine decarboxylase deficiency causes neural tube defects and features of non-ketotic hyperglycinemia in mice. *Nat. Commun.* **6,** 6388.

Pani,L., Horal,M., and Loeken,M.R. (2002). Rescue of neural tube defects in Pax-3-deficient embryos by p53 loss of function: implications for Pax-3-dependent development and tumorigenesis. *Genes Dev.* **16,** 676-680.

Piedrahita,J.A., Oetama,B., Bennett,G.D., Van Waes,J., Kamen,B.A., Richardson,J., Lacey,S.W., Anderson,R.G.W., and Finnell,R.H. (1999). Mice lacking the folic acid-binding protein Folbp1 are defective in early embryonic development. *Nature Genet.* **23,** 228-232.

Pryor,S.E., Massa,V., Savery,D., Greene,N.D.E., and Copp,A.J. (2012). Convergent extension analysis in mouse whole embryo culture. *Methods Mol. Biol* **839,** 133-146.

Reeves,F.C., Burdge,G.C., Fredericks,W.J., Rauscher,F.J., and Lillycrop,K.A. (1999). Induction of antisense Pax-3 expression leads to the rapid morphological differentiation of neuronal cells and an altered response to the mitogenic growth factor bFGF. *J. Cell Sci.* **112 (Pt 2),** 253-261.

Sah,V.P., Attardi,L.D., Mulligan,G.J., Williams,B.O., Bronson,R.T., and Jacks,T. (1995). A subset of *p53*-deficient embryos exhibit exencephaly. *Nature Genet.* **10,** 175-180.

Saitsu,H., Ishibashi,M., Nakano,H., and Shiota,K. (2003). Spatial and temporal expression of *folate-binding protein 1* (*Fbp 1*) is closely associated with anterior neural tube closure in mice. *Dev. Dyn.* **226,** 112-117.

Tibbetts,A.S. and Appling,D.R. (2010). Compartmentalization of Mammalian folate-mediated one-carbon metabolism. *Annu. Rev. Nutr.* **30,** 57-81.

Vousden,K.H. and Lane,D.P. (2007). p53 in health and disease. *Nat. Rev. Mol. Cell Biol.* **8,** 275-283.

Wlodarczyk,B.J., Tang,L.S., Triplett,A., Aleman,F., and Finnell,R.H. (2006). Spontaneous neural tube defects in splotch mice supplemented with selected micronutrients. *Toxicol. Appl. Pharmacol.* **213,** 55-63.

Zaganjor,I., Sekkarie,A., Tsang,B.L., Williams,J., Razzaghi,H., Mulinare,J., Sniezek,J.E., Cannon,M.J., and Rosenthal,J. (2016). Describing the Prevalence of Neural Tube Defects Worldwide: A Systematic Literature Review. *PLoS. One.* **11,** e0151586.

Figures

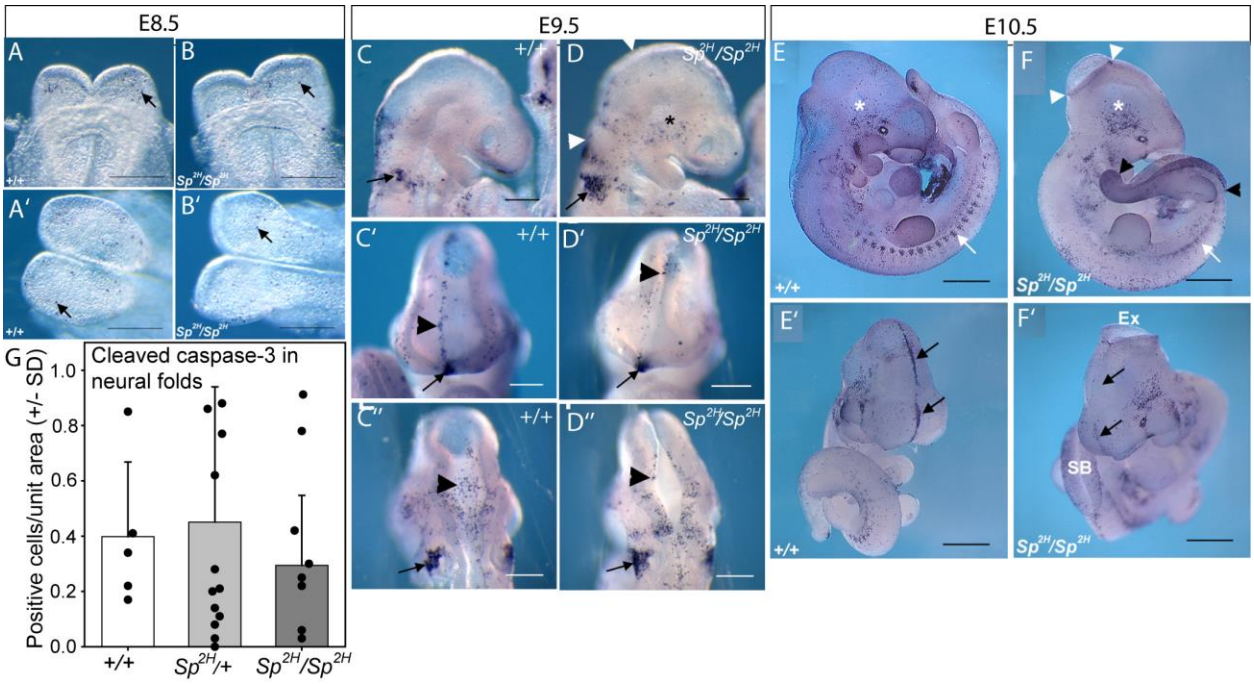

Figure 1. Apoptosis in the neuroepithelium is not affected by *Pax3* genotype. (A-F) TUNEL staining of embryos at E8.5 (A-B), E9.5 (C-D) and E10.5 (E-F) does not indicate any increase in the number of apoptotic cells in the neuroepithelium of *Pax3*$^{Sp2H/Sp2H}$ mutants (B, D, F), compared with wildtype (*Pax3*$^{+/+}$; A, C, E) embryos at the stages encompassing neural tube closure (A-B, ventral view; A'-B', dorsal view). The characteristic midline staining in the closed mid-forebrain of +/+ embryos (arrowhead in C', E') appears to be lacking in *Pax3*$^{Sp2H/Sp2H}$ embryos (D', F'), although staining at the rostral limit of the forebrain (anterior neural ridge) and lateral hindbrain (a site of neural crest cell migration) were present (black arrows in C-D). Scale bar represents 0.1 mm. (G) Quantitative analysis of cleaved caspase-3 immunostaining in the cranial neuroepithelium reveals no difference between genotypes. (Black circles represent single embryos with mean ± SD of this data shown in bars. Data for each embryo comprise 2-3 sections; overall 15-37 sections per genotype). See also Figure S1.

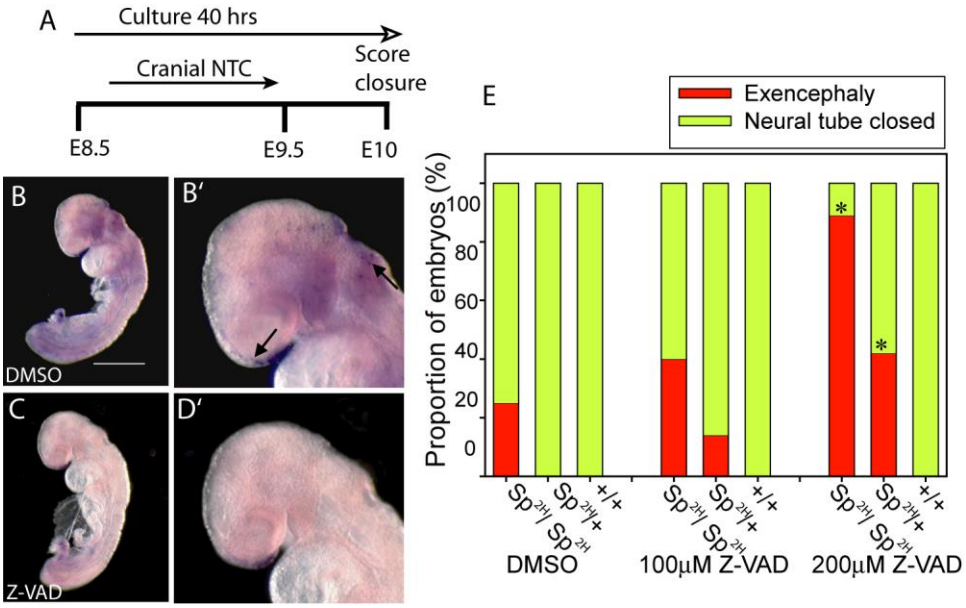

Figure 2. NTDs in *Pax3* mutant embryos are not prevented by apoptosis inhibition. Treatment of cultured embryos with Z-VAD-FMK (strategy in A) did not impede cranial neural tube closure in +/+ embryos (E) but led to increased frequency of exencephaly among *Pax3*$^{Sp2H/SpH}$ and *Pax3*$^{Sp2H/+}$ embryos compared with vehicle (DMSO) controls of the same genotype (* P<0.01; Fisher Exact test). TUNEL staining confirmed that apoptosis was suppressed in (C) Z-VAD treated embryos, compared to (B) vehicle-treated controls (apoptotic cells indicated by arrow in B'). N = 5-12 embryos per genotype for each treatment group (See Table S1 for numbers of embryos and measures of developmental progression and growth).

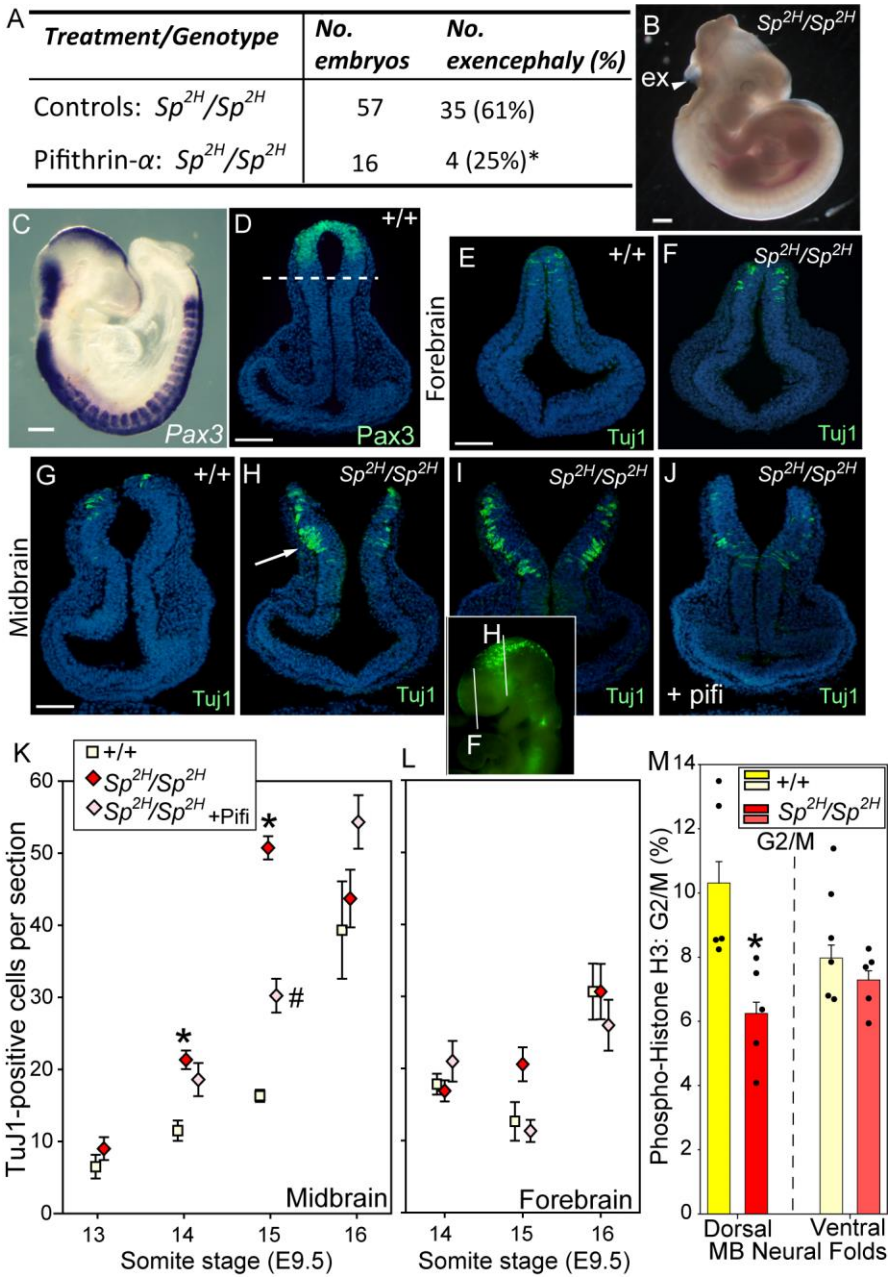

Figure 3. Premature neuronal differentiation and diminished proliferation in Pax3-mutant midbrain neuroepithelium. (A-B) Among *Pax3*$^{Sp2H/2H}$ embryos exposed to pifithrin-α (via maternal administration), the frequency of exencephaly (arrowhead in B) was significantly lower than among vehicle-treated controls (*p<0.02; Fisher Exact test). Data from 10 treated and 37 control litters, see Table S2 for additional details. Pax3 mRNA (C) and protein (D) are expressed in the dorsal neural tube (D, above dotted line on coronal section through the

midbrain). β-tubulin type III (Tuj1)-positive cells were analysed on coronal sections through the forebrain (E-F) and midbrain (G-J) at E9-9.5 (positions of sections in H and K shown on inset whole mount image). Scale bar represents 100 µm. (G-I, K) The midbrain neuroepithelium of *Pax3*$^{Sp2H/2H}$ embryos exhibits significantly more neuronal cells than in wild-type at the 14-15 somite stages (* indicates significant difference compared with wild-type embryos at same somite stage, P<0.002). (J-K) Pifithrin-α treatment results in significantly reduced number of TuJ1-positive cells in the midbrain of *Pax3*$^{Sp2H/2H}$ embryos at the 15 somite stage (# indicates significant difference compared with both +/+ and untreated *Sp*^{2H}/*Sp*^{2H} embryos, P<0.002). Each data point represents mean (± SEM) for 9-12 sections from a minimum of 3 embryos. (M) The proportion of PHH3-positive (late G2-M phase) cells was significantly lower in the dorsal neuroepithelium of the midbrain of *Pax3*$^{Sp2H/2H}$ embryos compared with +/+ littermates at E9.5 (14-15 somite stage; * P<0.01, ANOVA). Black circles (n = 5 embryos per genotype) represent single embryos with mean ± SEM of this data shown in bars (data for each embryo comprise 5 sections, n = 25 sections per genotype).

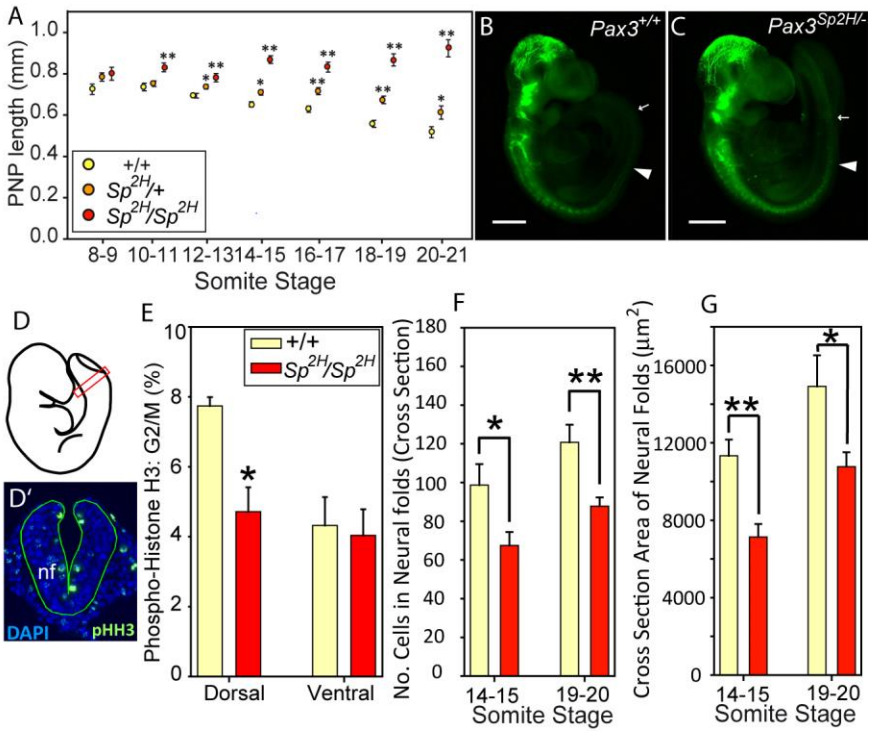

Figure 4. Diminished proliferation and altered dimensions in the spinal neural tube of *Pax3*$^{Sp2H/2H}$ embryos. (A) PNP length of *Pax3*$^{Sp2H/2H}$ embryos is enlarged from E9 (10-11 somite stage) onwards and delayed PNP closure is also evident in *Pax3*$^{Sp2H/+}$ embryos compared with stage-matched +/+ controls (*p<0.05, **p<0.01; ANOVA). (B-C) Staining for βIII-tubulin is detected in the spinal neural tube at E9.5 but the caudal limit (indicated by white arrowhead) does not approach the open PNP region (white arrow). See also Fig. S3. (D-G) Analysis of transverse sections (D') at the level of the closing neural folds (boxed in D) at E9.5 (14-15 somite stage) shows (E) a significantly lower proportion of PHH3-positive (late G2-M phase) cells in the Pax3-mutant dorsal neuroepithelium of *Pax3*$^{Sp2H/2H}$ compared with +/+ embryos (*P<0.01; t-test). The neuroepithelium of *Pax3*$^{Sp2H/2H}$ embryos displays a significantly lower number of cells (F) and cross-sectional area (G) than in +/+ embryos at both 14-15 and 19-20 somite stages (*P<0.05; **P<0.01). Bars in E-G represents mean ± SEM from 6 embryos per group (genotype and stage) with 5-6 sections per embryo (each bar corresponds to 32-36 sections).

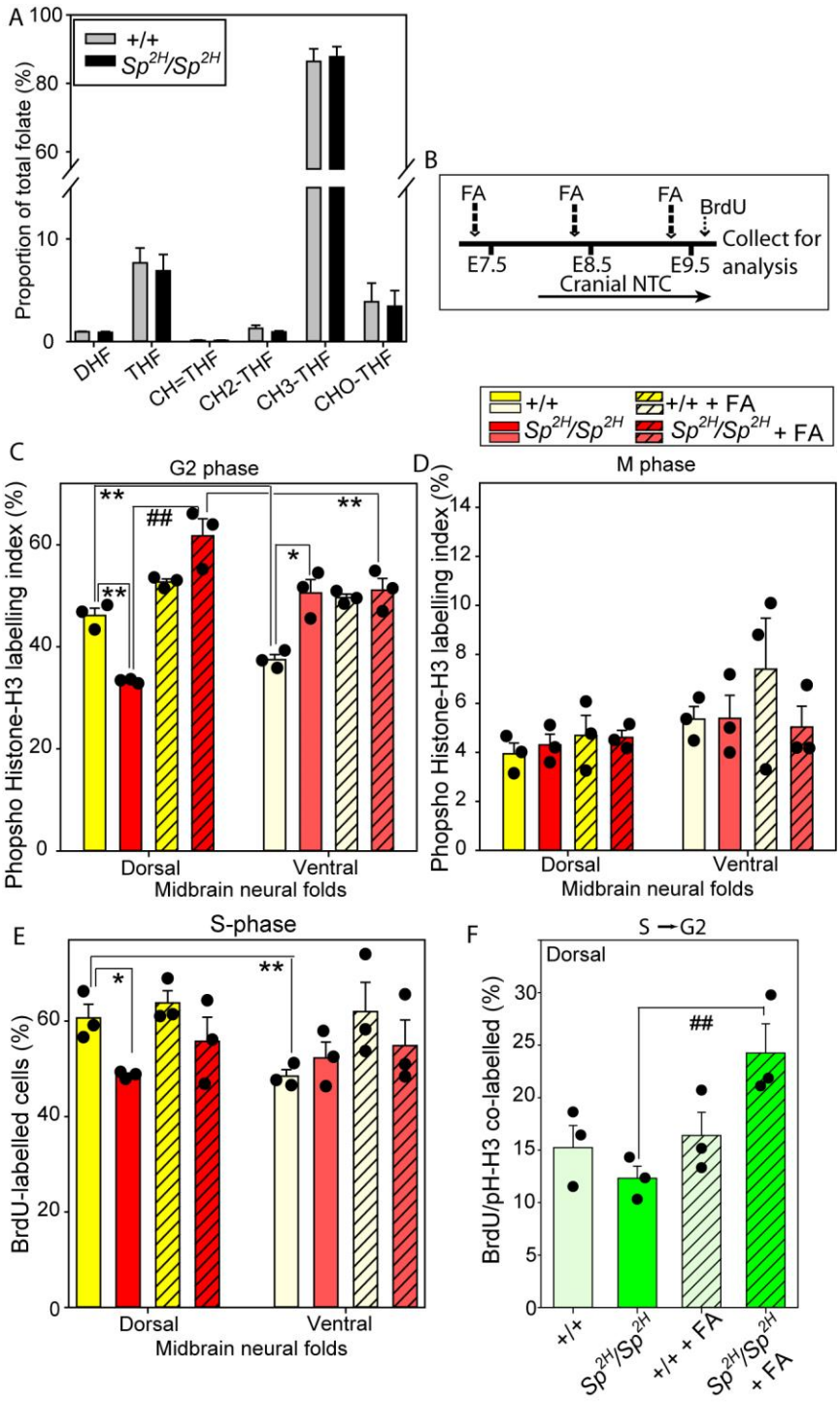

Figure 5. Folic acid promotes cell cycle progression in the Pax3 mutant neuroepithelium. (A) The relative proportion of differing folate species, separated by mass spectrometry, did not differ with genotype (DHF, dihydrofolate; THF, tetrahydrofolate; CH=THF, methenyl-THF;

CH2, methylene; CH3, methyl; CHO, formyl-THF)(n = 4 embryos per genotype). (B) Scheme for *in vivo* treatment with FA prior to embryo collection with analysis of the midbrain neuroepithelium for (C) PHH3 labelled cells in G2 phase, and (D) M-phase, or (E) BrdU labelling of S-phase. (F) Proportion of BrdU/PHH3 co-labelled cells in the dorsal neuroepithelium. Significant differences between genotypes, or between dorsal and ventral regions within treatment groups, are indicated (*P<0.025; **P<0.0025; ANOVA). FA treatment led to increased PHH3 (C) and PHH3/BrdU double labelling (F) in the dorsal neuroepithelium of *Pax3* mutants ($^{\#\#}$P<0.01; ANOVA).

Genotype	*No. embryos*	*No. exencephaly (%)*	*No. open PNP (%)*
Pax3 ; Trp53			
Sp^{2H}/Sp^{2H} ; +/+	5	4 (80%%)	3/3 (100%)
Sp^{2H}/Sp^{2H} ; +/-	24	12 (50%)	15/17 (88.2)
Sp^{2H}/Sp^{2H} ; -/-	9	8 (88.9%)	3/3(100%)
Sp^{2H}/+ ; +/+	31	0 (0%)	0/25 (0%)
Sp^{2H}/+ ; +/-	38	1 (2.6%)	0/23 (0%)
Sp^{2H}/+ ; -/-	26	9 (34.6%)*	2/19 (10.5%)
+/+ ; +/+	5	0 (0%)	0/2 (0%)
+/+ ; +/-	31	1 (3.2%)	1/25 (4%)
+/+ ; -/-	8	1 (12.5%)	0/4 (0%)

Table 1. Frequency of neural tube defects among offspring of $Pax3^{Sp2H/+}$:$Trp53^{+/-}$ intercrosses.

Litters were analysed at E10.5 for the presence of exencephaly (cranial NTDs) and/or a persistently open posterior neuropore (PNP) in embryos with 30 or more somites, which is indicative of incipient spina bifida. Cranial and spinal NTDs occurred at high frequency in $Pax^{Sp2H/Sp2H}$ embryos irrespective of *Trp53* genotype, arguing against a protective effect of p53 loss of function. Cranial NTDs were more frequent among in $Pax^{Sp2H/+}$ heterozygotes that lack p53 than in $Pax^{Sp2H/+}$ embryos that were wild-type for p53 (*$p<0.05$; z-test). Genotype frequencies did not depart significantly from Mendelian expectation ($p=0.34$; chi-square).

Supplementary Material

Treatment/ Genotype	*No.*	*Exen*	*PNP length (mm)*	*Somites*	*Crown-rump length (mm)*	*Yolk sac circulation*
Control-DMSO						
Sp^{2H}/Sp^{2H}	12	3 (25%)	1.21 ±0.16*	24.9 ±0.3	3.29 ±0.09	2.6 ±0.1
$Sp^{2H}/+$	15	0	0.46 ±0.06	25.3 ±0.3	3.36 ±0.07	2.4 ±0.2
+/+	8	0	0.36 ±0.06	25.3 ±0.5	3.40 ±0.11	2.6 ±0.2
100 μM ZVAD						
Sp^{2H}/Sp^{2H}	5	2 (40%)	0.90 ±0.13*	25.0 ±0.4	3.25 ±0.12	2.8 ±0.2
$Sp^{2H}/+$	7	1 (14%)	0.53 ±0.09	25.1 ±0.6	3.25 ±0.12	2.9 ±0.1
+/+	8	0	0.28 ±0.04	25.9 ±0.6	3.27 ±0.13	2.3 ±0.3
200 μM ZVAD						
Sp^{2H}/Sp^{2H}	9	8 (89%)#	0.97 ±0.13*	24.3 ±0.6	3.11 ±0.12	2.0 ±0.3
$Sp^{2H}/+$	12	5 (42%)#	0.55 ±0.05**	24.4 ±0.7	3.17 ±0.12	2.0 ±0.3
+/+	12	0	0.33 ±0.03	24.5 ±0.5	3.12 ±0.10	2.0 ±0.2

Table S1. NTD incidence, growth and development of *splotch* embryos cultured in the presence of ZVAD-FMK or DMSO only (vehicle control). Embryos were cultured for 40 hours from E8.5-10. No significant differences were detected in yolk-sac circulation score (ranked from 0: no circulation to 3: vigorous circulation throughout the yolk sac), crown-rump length or number of somites after culture, suggesting that there was # no adverse effect on viability, growth or developmental progression, respectively. Frequency of exencephaly (Exen) was signifcantly higher among embryos exposed to 200 μM ZVAD than among embryos of the same genotype exposed to DMSO ($p < 0.025$; Z-test).

* Mean posterior neuropore (PNP) lengths of Sp^{2H}/Sp^{2H} embryos were significantly larger than for heterozygous and wild-type embryos, reflecting the incipient spina bifida. ** The PNP was longer in $Sp^{2H}/+$ than in +/+ embryos and this was statistically significant in the 200 μM treatment group. No difference in PNP length was noted between treatment groups. Values are presented as mean ± SEM.

Treatment/Genotype	*No. litters*	*No. embryos*	*No. exencephaly (%)*	*No. spina bifida (%)*
Controls	37	225		
Sp^{2H}/Sp^{2H}		57	35 (61%)	20 (87%)
$Sp^{2H}/+$		106	0 (0%)	0 (0%)
+/+		62	1 (2%)	0 (0%)
Pifithrin-α	10	60		
Sp^{2H}/Sp^{2H}		16	4 (25%)*	14 (88%)
$Sp^{2H}/+$		27	0 (0%)	0 (0%)
+/+		17	0 (0%)	0 (0%)

Table S2. Incidence of neural tube defects among litters of *Splotch* (Sp^{2H}) mice treated with pifithrin-α. Dams were treated with pifithrin-α at E8.5 and E9.5, by intra-peritoneal injection at a dose of 0.22 mg/kg (10 µl/g of a 2.2 mg/ml stock solution), and controls were injected with the same volume of PBS. Litters were collected at E11.5 and analysed for the presence of neural tube defects. Mean litter size did not significantly differ between treatment groups.* Frequency of exencephaly is significantly lower among Sp^{2H}/Sp^{2H} embryos exposed to pifithrin-α than among PBS-treated ($p<0.05$; Z-test with Yates correction), whereas spina bifida frequency is not affected by pifithrin-α.

Developmental Stage	*No. litters*	*Genotype*	*No. embryos*	*Somite number*	*Crown-rump length (mm)*
E9.5	14	+/+	22	15.7 ± 0.5	2.2 ± 0.2
		Sp^{2H}/+	43	15.1 ± 0.2	2.1 ± 0.1
		Sp^{2H}/Sp^{2H}	23	15.9 ± 0.3	2.2 ± 0.1
E10.5	6	+/+	11	30.9 ± 0.8	4.3 ± 0.1
		Sp^{2H}/+	17	30.0 ± 0.5	4.1 ± 0.1
		Sp^{2H}/Sp^{2H}	8	30.3 ± 0.6	4.2 ± 0.1

Table S3. Number of somites and crown-rump length do not differ between *splotch* (Sp^{2H}) genotypes. Litters were collected at E9.5 and E10.5, the number of somites was counted and the crown-rump length measured using an eye-piece graticule. No significant differences between genotypes were detected at either stage of development. Values are presented as mean ± SEM.

Genotype/treatment	*No. embryos*	*No. exencephaly (%)*	*No. spina bifida (%)*
Formate	33		
Sp^{2H}/Sp^{2H}	5	3 (60.0%)	5 (100%)
$Sp^{2H}/+$	18	0 (0%)	0 (0%)
+/+	10	0 (0%)	0 (0%)
Controls	168		
Sp^{2H}/Sp^{2H}	37	25 (67.6)	35 (94.6%)
$Sp^{2H}/+$	70	0 (0%)	0 (0%)
+/+	31	0 (0%)	0 (0%)

Table S4. Frequency of neural tube defects among offspring of formate-treated mice.

Litters were generated by intercross of $Sp^{2H/+}$ mice. Dams were treated with formate (30 mg/ml in drinking water) and litters were analysed at E11.5 for the presence of exencephaly (cranial NTDs) and/or spina bifida.

Supplementary Figures

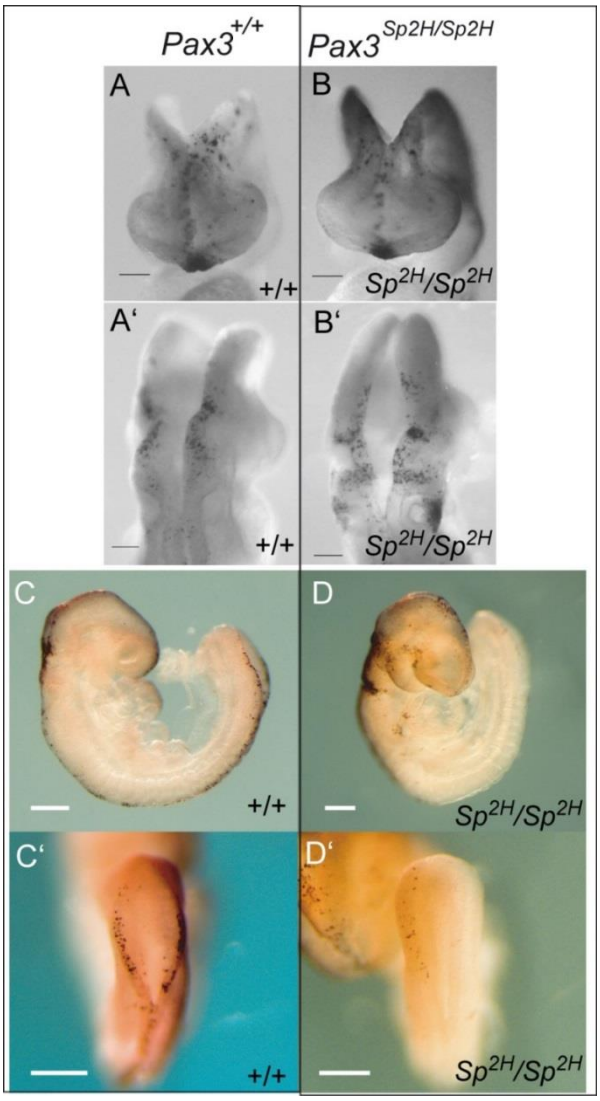

Figure S1. TUNEL staining of wild-type and *Pax3*$^{Sp2H/Sp2H}$ mutant embryos at E9.0. (A-B) No difference in numbers of TUNEL-positive apoptotic cells were detected in the neural folds of the cranial region (A, anterior view of forebrain; B, view of hindbrain). (C-D) There was no indication of excess TUNEL staining in the spinal region of *Pax3*$^{Sp2H/Sp2H}$ embryos, whereas some mutants exhibited fewer positive cells in the region of open spinal neural folds (compare D’ and C’). Scale bar represents 0.1 mm (A-B), 0.25 mm (C-D).

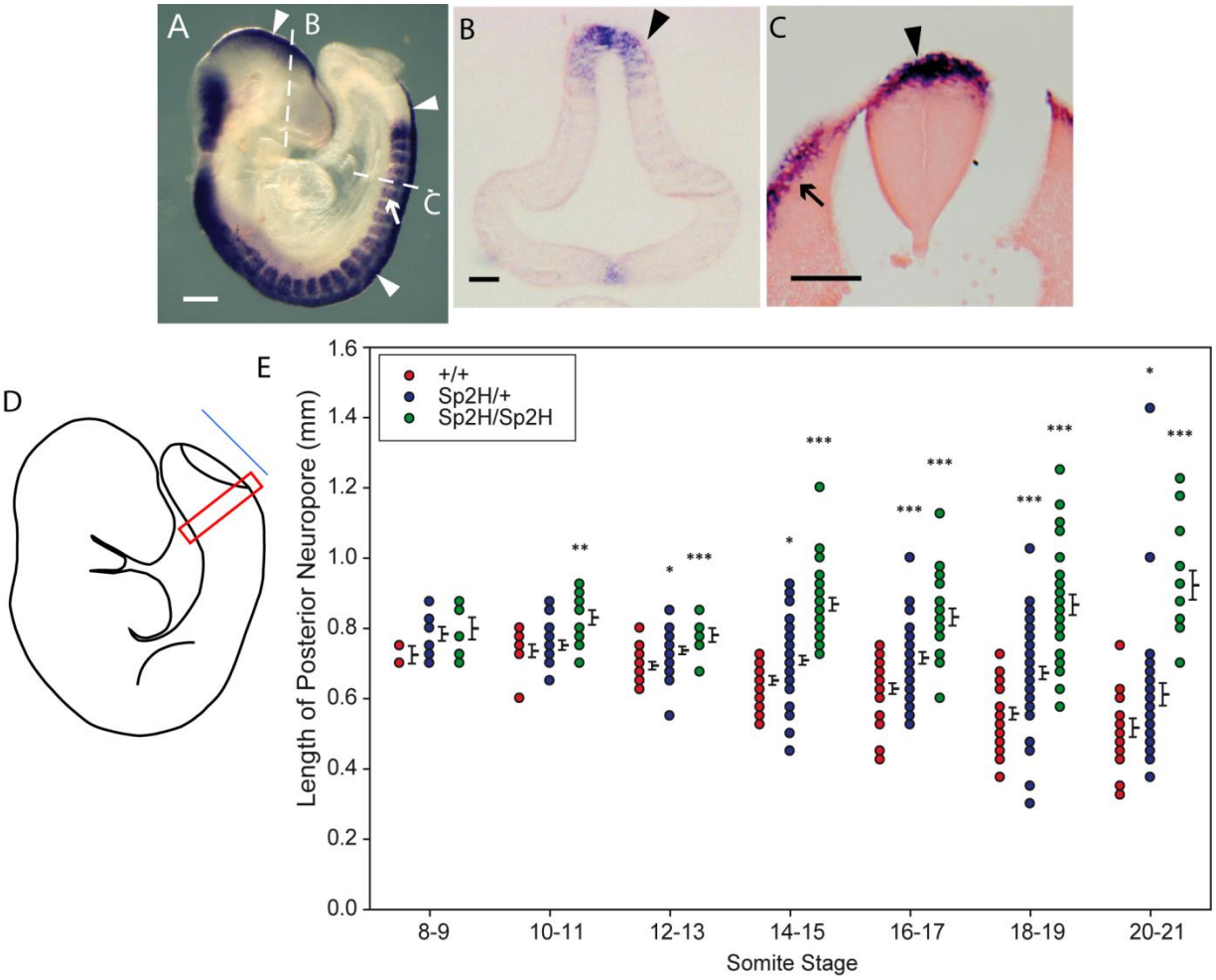

Figure S2. *Pax3* expression in the dorsal neural epithelium and failure PNP closure in *Pax3*$^{Sp2H/Sp2H}$ mutant embryos. (A-C) *In situ* hybridisation for *Pax3* shows expression in the dorsal neuroepithlium (arrowheads) in the cranial (B) and spinal (C) regions, as well as dermomyotome (arrow). (D-E) Raw data corresponding to Fig. 3A. Measurements of PNP length (indicated by blue line in D) show enlargement of PNP length in *Pax3*$^{Sp2H/2H}$ embryos from E9 (10-11 somite stage) onwards. Delayed PNP closure is also evident in *Pax3*$^{Sp2H/+}$ embryos compared with stage-matched +/+ controls (*p<0.05; **p<0.01; ***p<0.001; ANOVA).

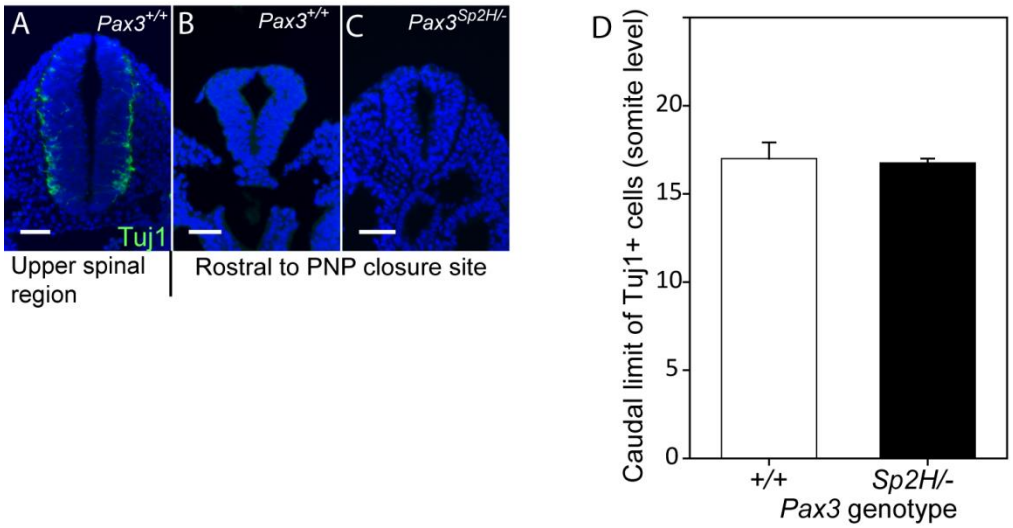

Figure S3. Neuronal differentiation does not occur at the level of PNP closure in wild-type or *Pax3* mutant embryos (related to Fig. 4). (A-C) Immunostaining for βIII-tubulin (Tuj1 in embryos at E9.5 (17-21 somite stage) confirms presence of positive cells at upper spinal levels (A) as seen in whole mount staining (Fig. 4B-C), whereas no positive cells are present the level of the recently closed neural tube rostral to the PNP closure site (B, C) in either wild-type or *Pax3* mutant embryos (images are representative of 3 embryos of each genotype; scale bar represents 50 µm). (D) The caudal-most limit at which βIII-tubulin (Tuj1) positive cells were detected was defined on the basis of the level of the somite adjacent to the neural tube. Among embryos at late E9.5 (23-24 somite stage), there was no significiant difference in the caudal level to which neuronal differentiation had progressed (n = 4 embryos per genotype).

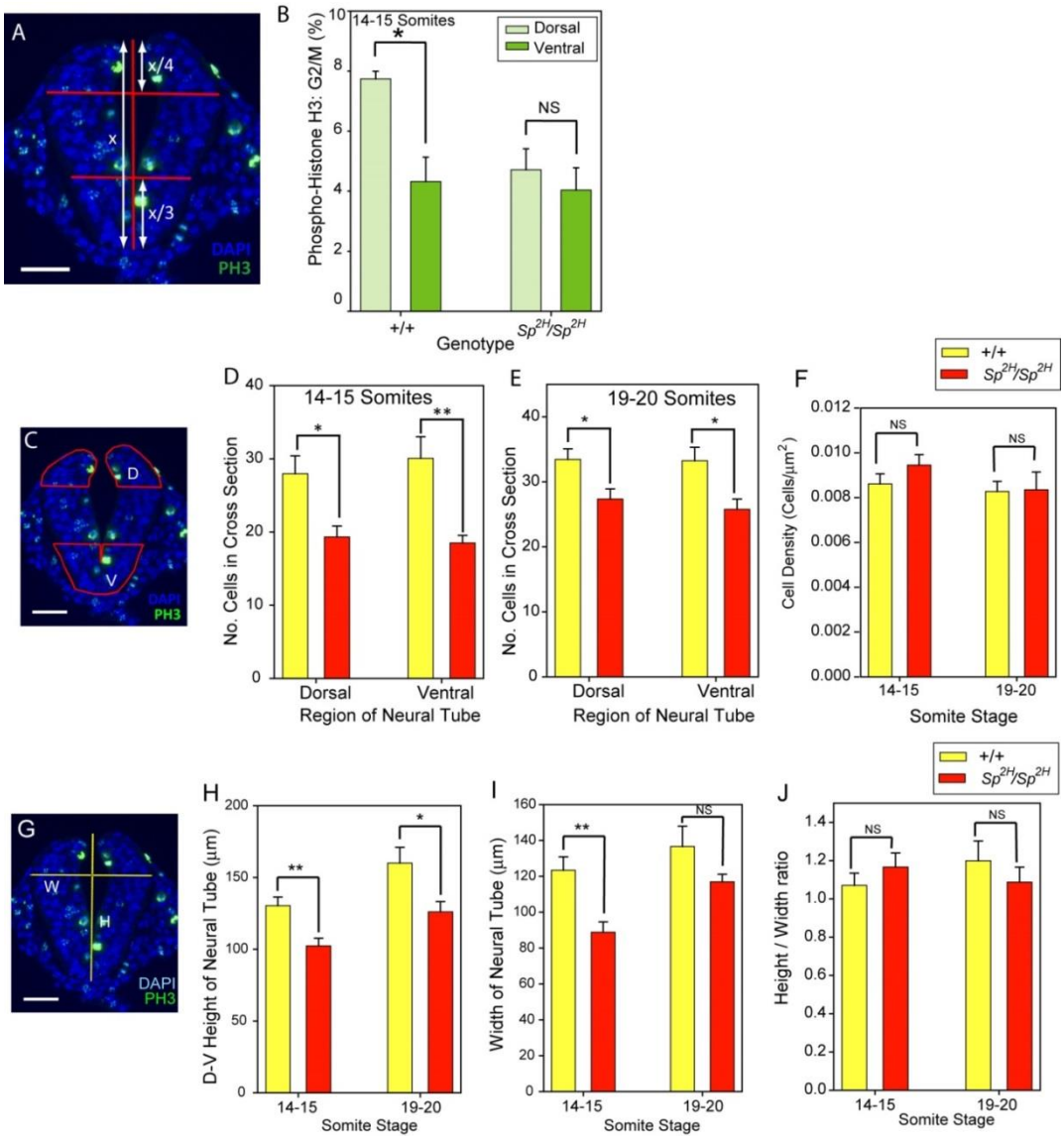

Figure S4. Analysis of proliferation, cell numbers and spinal neural tube size among wild-type and *Pax3*$^{Sp2H/Sp2H}$ mutant embryos at E9-9.5. (A-B) Immunostaining for PHH3 shows a significant dorsal-ventral difference in the number of cells at late G2-M phase in wild-type embryos (*P<0.05) but not in *Pax3* mutants (data re-plotted from Fig. 3). Dorsal and ventral regions used for analysis (A) correspond to Pax3-positive and negative regions, respectively. (C-E) The number of cells in transverse sections through the spinal neuroepithelium was lower in *Pax3*^{Sp2H} mutants than in +/+ embryos in both the dorsal and ventral regions (labelled D and V in panel C) at the 14-15 and 19-20 somite stages. (F) Overall cell density (cells/mm^2) did not differ between genotypes. (G-J) The dorsal-ventral height (H) and lateral width (W) of the spinal neuroepithelium was diminished in *Pax3*^{Sp2H} mutant embryos, but the height/width ratio did not differ from wild-type. (*P<0.05; **P<0.01; ANOVA); scale bars represent 50 µm. Bars represent mean ± SEM from 6 embryos per group (genotype and stage) with 5-6 sections per embryo (each bar corresponds to 32-36 sections).